

Publication II

A. Haarahiltunen, H. Talvitie, H. Savin, M. Yli-Koski, M. I. Asghar, and J. Sinkkonen. 2008. Modeling boron diffusion gettering of iron in silicon solar cells. *Applied Physics Letters*, volume 92, number 2, 021902, 3 pages.

© 2008 American Institute of Physics (AIP)

Reprinted by permission of American Institute of Physics.

Modeling boron diffusion gettering of iron in silicon solar cells

A. Haarahiltunen,^{a)} H. Talvitie, H. Savin, M. Yli-Koski, M. I. Asghar, and J. Sinkkonen
Helsinki University of Technology, P.O. BOX 3500, FI-02015 TKK, Finland

(Received 5 November 2007; accepted 17 December 2007; published online 14 January 2008)

In this paper, a model is presented for boron diffusion gettering of iron in silicon during thermal processing. In the model, both the segregation of iron due to high boron doping concentration and heterogeneous precipitation of iron to the surface of the wafer are taken into account. It is shown, by comparing simulated results with experimental ones, that this model can be used to estimate boron diffusion gettering efficiency of iron under a variety of processing conditions. Finally, the application of the model to phosphorus diffusion gettering is discussed. © 2008 American Institute of Physics. [DOI: 10.1063/1.2833698]

The diffusion of a high concentration of phosphorus is a well known gettering technique for removing detrimental transition metal contamination, such as iron, in silicon technology. In a silicon solar cell process, in which the starting material is often boron doped silicon, phosphorus diffusion gettering (P gettering) is naturally included in a process as the formation of the emitter. Jøge *et al.* have shown that in a bifacial solar cell with boron-diffused back surface field, gettering of iron by boron diffusion (B gettering) has also an important contribution to the final efficiency of the solar cell.¹ They also modeled the B gettering using so-called *iron behavior parameters* in silicon. In this paper, we propose a physical model for B gettering in silicon, which is based on the combination of segregation of iron to a heavily boron doped layer and heterogeneous precipitation of iron to the surface of the wafer.

We compare the reported experimental B-gettering results² with our simulations. Finally, we discuss the application of the model to P gettering.

In Refs. 3 and 4, we have presented a lumped model for heterogeneous precipitation of iron in silicon, which was used to model internal gettering. In Ref. 5, we used the same model to simulate of iron precipitation to boron implantation damage. The model assumes that the heterogeneous precipitation sites that already contain some iron are more attractive gettering sites than the ones with no iron, simply because of a lower chemical potential of iron in large precipitates. This assumption, together with the Fokker-Planck equation used to simulate the cluster evolution, leads to the model that includes the nucleation and growth of iron precipitates. In this letter, we use the model to simulate the iron precipitation to the wafer surface by adjusting the density of heterogeneous precipitation sites in a layer at the vicinity of the surface.

Diffusion and segregation of iron are simulated using an algorithm that is described in Ref. 6. The driving force for segregation is the chemical potential (supersaturation) gradient caused by the difference in solubility. The solubility of iron as a function of boron concentration is calculated as in Ref. 7. The maximum soluble concentration of neutral iron is expected to be independent of boron concentration. However, the solubility of total iron is enhanced by boron as there are additional positively charged iron ions as well as iron-

boron pairs. The effect on the diffusivity of iron through trapping of positively charged iron by boron is calculated, as suggested in Ref. 8.

We model iron precipitation to the surface of the wafer using parameters which we have found to be appropriate for internal gettering simulations,³ although some of the parameters might depend on the doping level or on the properties of the precipitation sites. In our model, the effect of boron doping on iron precipitation arises completely from the changes in solubility and diffusivity,

$$C_{\text{sol}}(\text{B}) = k_{\text{seg}}(\text{B})C_{\text{sol}},$$

$$D = D(\text{B}), \quad (1)$$

where C_{sol} is the solubility of iron in intrinsic silicon, D is the diffusion constant of iron, $k_{\text{seg}}(\text{B})$ is the segregation coefficient, $D(\text{B})$ is the effective diffusion constant of iron, and B is the boron concentration.⁵

Supersaturation is the driving force for nucleation of iron precipitates so the iron precipitation rate depends strongly on the initial supersaturation level.³ Together with Eq. (1), this means that heavy boron doping (i) decreases iron precipitation at constant iron contamination level as supersaturation decreases and (ii) increases iron precipitation at constant supersaturation level as the nucleation and growth rate increase due to higher iron concentration. The segregation strives for constant supersaturation through the whole wafer, thus, iron precipitation is faster in the region of heavier boron doping. However, the segregation always decreases the supersaturation. The strong reduction of the supersaturation can slow down or even prevent the precipitation completely everywhere in a wafer. In practice, this might happen if the segregation coefficient is very high and/or the volume of heavier boron doping is much larger than the volume of bulk doping as in conventional epitaxial wafers.

We test our model by analyzing the experimental results, which Terakawa *et al.* have reported in Refs. 2 and 9. The experimental details can be found from these references and only the essential parts are repeated here. Their experiments included studies of iron precipitation to the bare silicon surface (native oxide) at different contamination levels during isothermal annealing at 600 °C for various times. Particularly, they made a comparison between samples with and without 0.2 μm boron doped diffusion layer (B gettering) on

^{a)}Electronic mail: anti.haarahiltunen@tkk.fi.

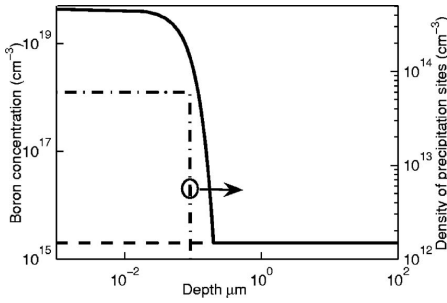


FIG. 1. The boron concentration and the density of heterogeneous precipitation sites as a function of depth, in our simulations. Solid line and dashed line represent the boron concentration with and without boron diffusion, respectively. Heterogeneous precipitation site density is adjusted to take precipitation of iron to the surface into account.

both wafer surfaces. They used B-doped ($2 \times 10^{15} \text{ cm}^{-3}$) Czochralski-grown silicon wafer whose thickness was $200 \mu\text{m}$.

The structures used in our simulations are illustrated in Fig. 1. We adjusted the boron diffusion profile to achieve the reported sheet resistivity of $280 \Omega/\square$ (Ref. 9) and thickness of $0.2 \mu\text{m}$. In the defect layer (Fig. 1), which takes into account the heterogeneous iron precipitation to wafer surfaces, we assume the radius of the heterogeneous precipitation sites to be 1 nm. The depth of the defect layer, 90 nm, was approximated based on the secondary ion mass spectrometry results,¹ which indicate that the surface precipitation occurs in a rather thin layer at the wafer surface. We assume the no-flux boundary condition at the depth of zero as well at the symmetry plane at $100 \mu\text{m}$ depth.

The experimental and our simulation results are presented in Fig. 2. Using the results from samples without B gettering and a structure presented in Fig. 1, we obtain a total density of iron precipitation sites of $6 \times 10^{13} \text{ cm}^{-3}$. Firstly, it is important to note that in simulations, the parameters of the

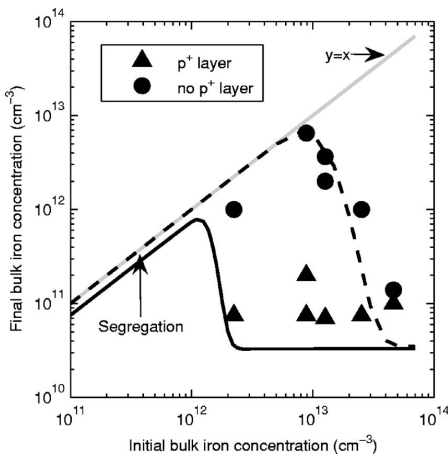


FIG. 2. The final bulk iron concentration as a function of initial iron concentration is shown after 600°C anneal for 2.25 h. Triangles and circles are the experimental results (taken from Ref. 2) with and without boron doped p^+ layer, respectively. Solid line and dashed line are the corresponding simulation results. The curve $y=x$ is used as a reference to illustrate the effect of gettering.

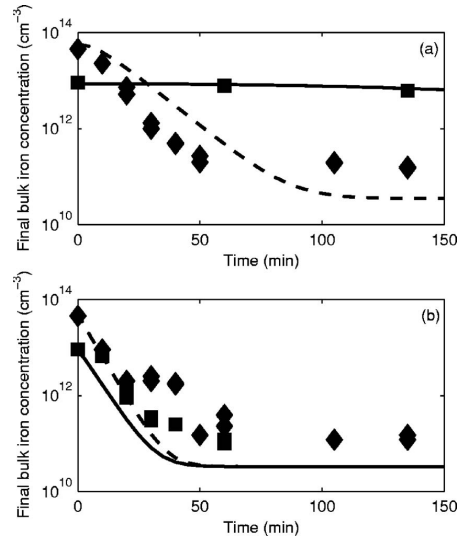


FIG. 3. The time evolution of final bulk iron concentration is illustrated in a wafer (a) without and (b) with boron doped p^+ layer. Squares and diamonds are experimental results (taken from Ref. 2) of low ($\approx 9 \times 10^{12} \text{ cm}^{-3}$) and high ($\approx 5 \times 10^{13} \text{ cm}^{-3}$) initial iron concentration, respectively. Solid line and dashed line are simulation results of low and high initial iron concentration, respectively.

defect layer, i.e., the width and the precipitation site density and radius, are kept constants and the difference between results in Fig. 2 arises entirely from segregation of iron to the boron doped p^+ layer. Secondly, the total density of precipitation sites depends on the surface preparation/conditions, e.g., it has been reported⁸ that a high quality oxide layer prevents or slows down iron out diffusion.

Terakawa *et al.* proposed that the critical iron contamination level for the formation of the iron rich silicon layer, i.e., nucleation and growth of iron precipitates, to the wafer surface is lower in the case of heavy boron doping.² However, our model proposes exactly the opposite effect; the critical contamination level increases in the case of heavy boron doping as the solubility increases. Nevertheless, the experimental and simulation results have a quite natural explanation. The boron doped p^+ is very thin compared to the bulk of the wafer. Thus, the supersaturation in the wafer is decreased only by a very small amount due to the iron segregation to the boron doped p^+ layer. This decrease in supersaturation, which is illustrated by an arrow in Fig. 2, is more than compensated by the fact that the nucleation and growth rate of iron precipitates are increased by a factor $D(B)k_{\text{seg}}(B) (\gg 1)$ as the segregation increases iron concentration in the thin boron doped p^+ layer.

Figure 3 shows the fact that our simulations also capture the experimental results of the time evolution of gettering to a reasonable accuracy. The results show clearly a time lag induced by nucleation and initial growth stage of iron precipitates without the boron doped p^+ layer [Fig. 3(a)], while in case of boron doped p^+ layer, the time evolution is much faster [Fig. 3(b)].

We can use the above mentioned precipitation/segregation model to optimize iron gettering in single crystal silicon if we know the boron concentration profile. The simu-

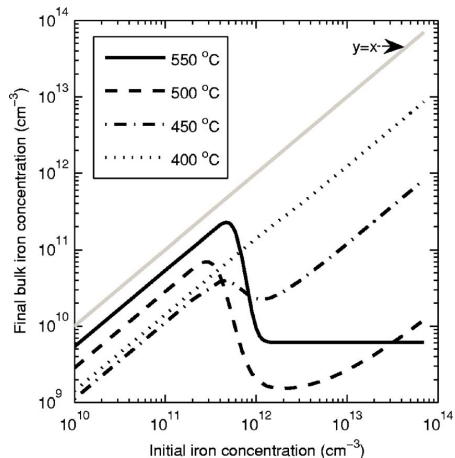


FIG. 4. (Color online) The final bulk iron concentration as a function of initial iron concentration is shown at various temperatures for isothermal 2.25 h anneal. The curve $y=x$ is used as a reference to illustrate the effect of gettering.

lation results in Fig. 2 indicate that 2.25 h gettering treatment at 600 °C is effective only at contamination levels above $2 \times 10^{12} \text{ cm}^{-3}$. In order to find optimum temperature for gettering of contamination levels below $2 \times 10^{12} \text{ cm}^{-3}$, we made a series of simulations in which the duration of the anneal was kept constant (2.25 h) but the temperature was varied (Fig. 4).

We can see that the optimum gettering temperature depends on the contamination level and the optimum gettering temperature is around 500 °C if the initial contamination level is between 5×10^{11} and $3 \times 10^{13} \text{ cm}^{-3}$. Within this contamination range, it is still possible to get some benefits from iron precipitation and, indeed, the gettering process is rather robust. However, if the contamination level is below $1 \times 10^{11} \text{ cm}^{-3}$, it is better to increase the segregation coefficient by decreasing the gettering temperature to the range of 400–450 °C. At lower temperatures, diffusion limits the gettering and rather long annealing times are needed to further improve the gettering efficiency. At 400 °C, iron does not precipitate at any contamination level as 2.25 h annealing is too short for iron to accumulate into the boron doped p^+ layer, i.e., supersaturation (concentration) in the boron doped p^+ layer remains too low for the nucleation of iron precipitates. The short annealing time also explains why the effect of segregation is slightly weaker at 400 °C than at 450 °C although the segregation coefficient increases as temperature decreases.

We present here only the results of B gettering as a quantitative model^{7,8} for segregation coefficient of iron in case of boron doped layer is well established. Actually, Weber *et al.* have demonstrated that the segregation coefficient of iron to heavily boron doped silicon is sufficiently large to explain the high temperature gettering at 940 and 990 °C.¹⁰ Terakawa *et al.* pointed out that segregation alone cannot explain their experimental results and they used surface precipitation as an explanation for the observed gettering.² However, they completely neglected the effect of segrega-

tion, which certainly took place under the used experimental conditions.

Improved P gettering using a low temperature annealing after phosphorus diffusion has been proposed in several publications.^{11–13} This clearly indicates that iron precipitation, as directly proposed and demonstrated by Buonassisi *et al.*,¹³ is also important in P gettering. The problem is that the segregation coefficient of iron to phosphorus doped layer is not well known. Istratov *et al.* have assumed the segregation coefficient to be equal to the segregation coefficient of similarly doped boron layer.⁷ Seibt *et al.* have used the properties of cobalt to calculate the iron segregation to phosphorus doped layer in their P-gettering simulations.¹⁴ We propose that the model presented here along with the known segregation coefficient, which should be determined from independent experiments, e.g., using epitaxial n^+p wafers, can be used to model P gettering.

In conclusion, we propose an improved model for B and P getterings of iron in silicon. The model includes segregation to gettering layer and precipitation of iron to the surface of the wafer. The simulation results show that the model can be used to explain the results of low temperature B gettering, which cannot be explained by segregation alone. In the case of P gettering, the model gives an explanation for the beneficial effect of a low temperature gettering.

O. Anttila from Bullen Semiconductor Corp. is acknowledged for helpful discussion. This work was financially supported by the Finnish National Technology Agency, Academy of Finland, Okmetic Oyj, Micro Analog Systems Oy, and VTI Technologies Oy.

¹T. Joge, I. Araki, T. Uematsu, T. Warabisako, H. Nakashima, and K. Matsukuma, *Jpn. J. Appl. Phys., Part 1* **42**, 5397 (2003).

²T. Terakawa, D. Wang, and H. Nakashima, *Jpn. J. Appl. Phys., Part 1* **45**, 2643 (2006).

³A. Haarahiltunen, H. Väinölä, O. Anttila, M. Yli-Koski, and J. Sinkkonen, *J. Appl. Phys.* **101**, 043507 (2007).

⁴A. Haarahiltunen, H. Väinölä, O. Anttila, E. Saarnilehto, M. Yli-Koski, J. Storgårds, and J. Sinkkonen, *Appl. Phys. Lett.* **87**, 151908 (2005).

⁵A. Haarahiltunen, H. Talvitie, H. Savin, O. Anttila, M. Yli-Koski, M. I. Asghar, and J. Sinkkonen, *J. Mater. Sci.: Mater. Electron.* (submitted), Special Issue DRIP-XII Conference 2007.

⁶H. Hieslmair, S. Balasubramanian, A. A. Istratov, and E. R. Weber, *Semicond. Sci. Technol.* **16**, 567 (2001).

⁷A. A. Istratov, W. Huber, and E. R. Weber, *J. Electrochem. Soc.* **150**, G244 (2003).

⁸H. Kohno, H. Hieslmair, A. A. Istratov, and E. R. Weber, *Appl. Phys. Lett.* **76**, 2734 (2000).

⁹T. Terakawa, D. Wang, and H. Nakashima, *Jpn. J. Appl. Phys., Part 1* **44**, 4060 (2005).

¹⁰T. Weber, C. Zechner, D. Macdonald, and P. P. Altermatt, in *Proceedings of the 21st European Photovoltaic Solar Energy Conference (EUPVSEC)*, Dresden, Germany, edited by J. Poortmans, H. Ossenbrink, E. Dunlop, and P. Helm (WIP-Renewable Energies, 2006), pp. 1486–1489.

¹¹J. Härkönen, V.-P. Lempiäinen, T. Juvonen, and J. Kylmäluoma, *Sol. Energy Mater. Sol. Cells* **73**, 125 (2002).

¹²P. Manshanden and L. J. Geerligs, *Sol. Energy Mater. Sol. Cells* **90**, 998 (2006).

¹³T. Buonassisi, M. D. Pickett, and R. Sweeney, in *Proceedings of 17th Workshop on Crystalline Silicon Solar Cells and Modules: Materials and Processes*, Vail, Colorado, edited by B. L. Sopori (National Renewable Energy Laboratory, Golden, Colorado, 2007), pp. 218–221.

¹⁴M. Seibt, A. Sattler, C. Rudolf, O. Voß, V. Kveder, and W. Schröter, *Phys. Status Solidi A* **203**, 696 (2006).